Multiscale Enrichment based on Partition of Unity

Jacob Fish and Zheng Yuan
Departments of Civil, Mechanical and Aerospace Engineerinh
Rensselaer Polytechnic Institute
Troy, NY 12180, USA
fishj@rpi.edu

Abstract

A new Multiscale Enrichment method based on the Partition of Unity (MEPU) method is presented. It is a synthesis of mathematical homogenization theory and the Partition of Unity method. Its primary objective is to extend the range of applicability of mathematical homogenization theory to problems where scale separation may not be possible. MEPU is perfectly suited for enriching the coarse scale continuum descriptions (PDEs) with fine scale features and the quasi-continuum formulations with relevant atomistic data. Numerical results show that it provides a considerable improvement over classical mathematical homogenization theory and quasi-continuum formulations.

1. Introduction

This manuscript is concerned with developing a systematic approach aimed at enriching coarse scale mathematical models with relevant fine scale features. The fine scale enrichment could be either discrete (atomistic) or continuous. The discrete variant of the enrichment is designed to enrich quasi-continuum formulations, whereas the continuum enrichment is targeted for coarse scale models governed by PDEs.

The method advocated in this paper belongs to the category of methods employing hierarchical decomposition of the approximation space in the form of $u = u^c + u^f$, where u^c and u^f are coarse and fine scale solutions, respectively. The literature on this type of methods is rapidly expanding, in particular due to the renewed interest in scale bridging methods spurred by the emergence of nanotechnology.

There seems to be no consensus on the origin of this decomposition, but quite often the global-local paper of Mote [1] that appeared in 1971 is mentioned in this regard in finite elements. For review articles on the early attempts in mid and late 70s see Noor [2] and Dong [3]. In most of these early attempts global functions describing closed form analytical solutions (u^f), such as crack tip asymptotic fields [4] or discontinuities in shear bands [5], were used to enrich finite element approximations (u^c). These so-called Global Enrichment Methods (GEM)

are very efficient in enhancing finite element discretizations with very few fine scale functions known to approximately describe the asymptotic behavior of the solution, but on the negative side, they often result in dense matrices.

These considerations spurred the development of Local (element level) Enrichment Methods (LEM) where the fine scale function(s) can be condensed out on the element level. Local enrichment functions have been used to embed discontinuous strains [6,7], curvatures [8] and displacements [9,10]. Variational Multiscale Method (VMS) [11] fall into this category of methods. VMS was partially motivated by identifying it with classical stabilized methods where u^f takes the form of a residual-free bubble [12,13]. These bubbles are functions required to vanish on element boundaries for second order problems. VMS has been subsequently applied to embed micromechanical fields in solid mechanics by Garikipati and Hughes [14,15].

Mathematical Homogenization [16,17,18] can be interpreted as a Local Enrichment Method. By this approach $u^c = u^0(x)$ and $u^f = \zeta u^1(x,y) + O(\zeta^2)$, where x and $y = x/\zeta$ are coarse and fine scale position vectors, respectively; $0 < \zeta = l/L \ll 1$, and l, L denote the characteristic size of the fine and coarse scales, respectively. Note that the leading order fine scale solution is $O(\zeta)$, whereas the leading order solution gradient (or strain), $\varepsilon^0 = \nabla_x^s u^0 + \nabla_y^s u^1$, has $O(1)$ contribution from both the fine and coarse scales, where ∇_x^s, ∇_y^s are symmetric gradient with respect to the coarse and fine scale coordinates, respectively, and ε^0 is the leading order strain. Moreover, since the fine scale is related to the coarse scale by $\nabla_y^s u^1 = \phi(y)\, \nabla_x^s u^0(x)$ it can be eliminated at the level of the coarse scale material point (constitutive equation) by means of homogenized or effective material properties.

An attractive feature of the Local Enrichment Methods is that fine-scale features can be eliminated either on the coarse scale element level (static condensation) or at the coarse scale material point (effective properties) resulting in embedded fine-scale physics at the coarse scale without significantly increasing the cost of coarse scale computations. On the negative side, fine scale features are only approximated, and their gross response is injected into the coarse scale. This type of scale bridging is often coined as sequential, serial, information-passing, or parameter-passing.

The need to control fine scale approximations without compromising the sparsity of discrete approximations produced several enrichment schemes to be referred here as Sparse Global Enrichment Methods (SGEM). Among the noteworthy SGEMs are the s-version of the finite element method [19,20,21,22] with application to strong [23,24] and weak [25,26,27,28] discontinuities, various multigrid-like scale bridging methods [29, 30, 31, 32], the Extended Finite Element Method (XFEM) [33,34,35] and the Generalized Finite Element Method (GFEM) [36,37] both based on the Partition of Unity (PU) framework [38,39] and the Discontinuous Galerkin (DG) [40,41] method. Multiscale methods [19-41] based on the concurrent resolution of multiple scales are often called as embedded, concurrent, integrated or hand-shaking multiscale methods.

In the s-version, the fine grid is superimposed in subdomain(s) where fine scale resolution is needed. It offers the flexibility of retaining fixed coarse grid, while adapting the fine grid based on where and when is required. The downside is the need for remeshing the fine grid and somewhat cumbersome quadrature required to integrate coupling terms between the meshes. Unstructured multigrid-like methods require remeshing to capture evolving fine scale features, but the need for integrating coupling terms is circumvented. Multigrid-like approaches aimed at bridging between discrete and continuum scales have been reported in [32,42,43].

The attractiveness of PU-based methods stems from the fact that special functions known to approximate the solution can be embedded into the coarse scale by a simple multiplication of these functions with standard finite element shape functions without introducing finer grids. The PUM-based methods are based on the theorem [38], which states that if there exist such a enrichment function ψ_α known to approximate the exact solution u^{ex} on a patch Ω_α, such that $\sum_i \left\| u^{ex} - \psi_\alpha \right\|^2_{\mathcal{U}(\Omega_\alpha)} \le \xi^2$, then the global error is bounded by $\left\| u^{ex} - \sum_\alpha N_\alpha \psi_\alpha \right\|_{\mathcal{U}(\Omega)} \le \xi$, where N_α and ψ_α are the standard finite element shape functions and special functions known to approximate the solution on a patch.

Special functions can be also introduced locally using Lagrange multipliers [44] or by means of the Discontinuous Galerkin method [40], but the question of stability cannot be easily resolved, and the implementation of such methods requires major changes to existing finite element codes.

In XFEM, which use local Partition of Unity [45], the enrichment functions are used to describe spatial features, such as asymptotic crack fields [33] or local flow fields [46]; in addition they provide means to model arbitrary discontinuities. For this discontinuous enrichment functions, the problem of linear dependency does not arise, but the issue of ensuring the integration errors to be significantly smaller than the approximation errors requires special attention [35]. In GFEM, which uses special handbook function [36,37], the resulting space is not linearly independent and the computational overhead (needed for either reorthogonalization or for using an indefinite solver) might be quite significant. Moreover, integration of coupling terms involving special handbook functions is challenging at best, and therefore it is not surprising that the method has been implemented for two dimensional problems only.

The method presented in this manuscript is a synthesis of the mathematical homogenization theory [16, 17] and the Partition of Unity method. It is intended for class of problems involving multiple spatial scales. One of the main objectives of the so-called Multiscale Enrichment based on Partition of Unity (MEPU) method is to extend the range of applicability of the mathematical homogenization theory to problems where scale separation may not exist, i.e., beyond the traditional range of $\zeta = l / L \ll 1$. MEPU is applicable to both enriching coarse scale continuum description with fine scale (computationally unresolvable) features as well quasi-continuum formulations [47,48] with relevant atomistic data. The latter can be viewed as an atomistically informed (and therefore nearly optimal) generalization of the classical Born rule.

MEPU takes advantage of the simplicity of the information transfer between the scales inherent to the mathematical homogenization theory and the elegance of enforcing C^0 continuity of solution without compromising on sparsity provided by the Partition of Unity framework. MEPU is free of some of the drawbacks inherent in each of its two constituents, namely: (i) the discontinuity of the fine scale enrichment function $\zeta u^1(x,y)$ resulting from the mathematical homogenization theory and (ii) some challenges involved in integrating coupling scale terms appearing in PU based methods. Moreover, MEPU is a hierarchical method in the sense that it converges to the fine scale description as the space of enrichment functions is expanded and the size of the coarse mesh is decreased. Therefore, it could serve as a dual-purpose concurrent - information-passing method.

The outline of this paper is as follows. Section 2 describes the basic formulation of the method. Analysis of the accuracy of the integration scheme is given in Section 3. The issue of interfacing MEPU and standard elements is studied in Section 4. Validation studies for continuum and quasi-continuum problems are given in Section 5. Conclusions and future research directions are outlined in Section 6. Attention is restricted to linear constitutive equations (or harmonic potentials) and steady state problems.

2. Formulation of MEPU

We start by stating the key result from the mathematical homogenization theory for periodic elastic heterogeneous media. Consider a two-term double-scale asymptotic expansion of the solution, $u_i = u_i^0(\boldsymbol{x}) + \zeta u_i^1(\boldsymbol{x},\boldsymbol{y})$, where $\boldsymbol{x}$ and $\boldsymbol{y} = \boldsymbol{x}/\zeta$ are coarse and fine scale position vectors, respectively; $0 < \zeta = l/L \ll 1$, and l, L denote characteristic size of the fine and coarse scale, respectively. Following [16,17,18] the fine scale solution is given as

$$u_i^1(\boldsymbol{x},\boldsymbol{y}) = \chi_{ikl}(\boldsymbol{y})\varepsilon_{kl}^0(\boldsymbol{x}) \tag{1}$$

where lower case Roman subscripts are reserved for spatial dimensions; ε_{ij}^0 the symmetric gradient of the coarse scale solution given by $\varepsilon_{ij}^0 \equiv u_{(i,j)}^0 = (u_{i,j}^0 + u_{j,i}^0)/2$; comma denotes the spatial derivative; regular brackets around two subsripts denote symmetric gradient; and $\chi_{ikl}(\boldsymbol{y})$ is the influence function (symmetric with respect to *kl* indices) obtained from the unit cell solution, the continuum version of which is given by:

$$\begin{aligned} &\frac{\partial}{\partial y_j}\left[L_{ijkl}\left(\chi_{(i,j)kl} + I_{ijkl}\right)\right] = 0 \;\; on \;\; \Theta \\ &\chi_{ikl}(\boldsymbol{y}) = \chi_{ikl}(\boldsymbol{y} + \hat{\boldsymbol{y}}) \quad on \quad \partial\Theta \\ &\chi_{ikl}(\boldsymbol{y}) = 0 \;\; on \quad \partial\Theta^{vert} \end{aligned} \tag{2}$$

where Θ is a unit cell domain, $\partial\Theta$ is its boundary and $\partial\Theta^{vert}$ are the vertices of the unit cell; L_{ijkl} - the linear elasticity constitutive tensor, $I_{klmn} = \left(\delta_{mk}\delta_{nl} + \delta_{nk}\delta_{ml}\right)/2$; $\hat{\boldsymbol{y}}$ is the basic period of the unit cell; Eq (2)c is often replaced by the normalization condition $\int_\Theta \chi_{ikl} d\Theta = 0$. The unit cell problem is typically solved using finite element method.

One of the salient features of the mathematical homogenization theory is that the fine scale solution is completely described by the coarse scale and that the influence functions can be precomputed at a material point. The microstructure in the unit cell could be periodic or random, but the solution has to be locally periodic, i.e., at the neighboring points in the coarse mesh, homologous by periodicity (same $\hat{\boldsymbol{y}}$), the value of a response function is the same, but at points corresponding to different points in the coarse scale (different $\boldsymbol{x}$), the value of the function can be different.

For these assumptions to be valid a unit cell has to "experience" a constant variation of ε_{ij}^0 over its domain Θ. This assumption breaks down in the high gradient regions, such as in the vicinity of cracks or cutouts or where the characteristic size of the unit cell is comparable to the coarse scale features. To allow for variation of the coarse scale solution over the unit cell domain, MEPU removes the dependency of the fine scale functions on the coarse scale solution by replacing ε_{ij}^0 and $\zeta\chi_{ikl}(\boldsymbol{y})$ in Eq. (1) with an independent set of degrees-of-freedom $a_{ij\alpha}$ and the influence functions defined over the local supports $\chi_{ikl}(\boldsymbol{x})N_\alpha(\boldsymbol{x})$, respectively. It is convenient to replace a pair of subscripts kl in χ_{ikl} and $a_{kl\alpha}$ denoting the enrichment mode by a single upper case Roman subscripts, A, i.e. $\chi_{ikl} \rightarrow \chi_{iA}$ and $a_{kl\alpha} \rightarrow a_{A\alpha}$. The resulting solution approximation states

$$u_i = \underbrace{N_\beta(\boldsymbol{x})d_{i\beta}}_{u_i^0} + \chi_{iA}(\boldsymbol{x})N_\alpha(\boldsymbol{x})a_{A\alpha} \tag{3}$$

where summation convention is employed for the repeated indices; Greek subscripts denote finite element nodes.

The discrete system of equations is obtained using a standard Galerkin method. MEPU exploits the special structure of the influence functions by utilizing Homogenization-Like Integration (HLI) scheme. The accuracy of the integration scheme is studied in Section 3. Let $I = \int_{\Omega^e} f d\Omega$ be a typical integral to be evaluated over the element domain Ω^e, then the Homogenization-Like Integration scheme states:

$$I = \int_{\square} J f d\square = \sum_{I=1}^{ngauss} W_I J_I f_I = \sum_{I=1}^{ngauss} W_I J_I \underbrace{\frac{1}{|\Theta|}\int_{\Theta_I} f d\Theta}_{f_I} \tag{4}$$

where $\square$ is the biunit parent domain, J the Jacobean, and *ngauss* the number of quadrature points.

The HLI scheme schematically depicted in Figure 1, centers a unit cell at each of the coarse scale Gauss points. The value of the integrand at a coarse scale Gauss point is replaced by its integral over the unit cell domain normalized by the volume of the unit cell. For coarse scale elements, encompassing numerous unit cells there is a significant cost savings compared to the

direct numerical integration over all unit cells contained in the coarse scale element. Moreover, direct numerical integration difficulties caused by intersecting coarse scale element boundaries with unit cell boundaries are automatically resolved by HLI.

Compared to the classical homogenization theory, there is an overhead associated with: (i) additional degrees-of-freedom, $a_{A\alpha}$, which cannot be condensed out on the element level, and (ii) the need for integration over all the coarse scale Gauss points as opposed to a single integration over the unit cell domain required by the classical homogenization theory for linear problems. Ideally, MEPU should be used in the critical regions only, whereas the classical homogenization should be employed elsewhere. The issue of transitioning between the two regions is discussed in Section 4.

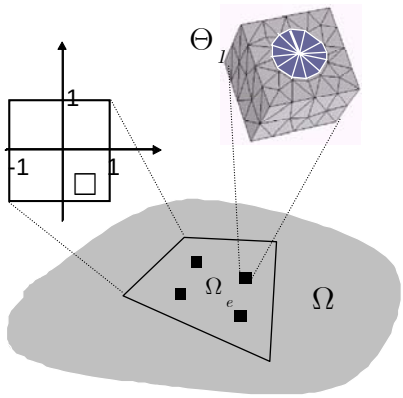

Figure 1: Homogenization-like integration scheme

Remark 1: MEPU can be generalized to quasi-continuum as follows. The starting point is the asymptotic expansion $u_i = u_i^0(\boldsymbol{x}) + \zeta u_i^1(\boldsymbol{x}, \boldsymbol{y})$ and $u_i^1(\boldsymbol{x}, \boldsymbol{y}) = \chi_{iA}(\boldsymbol{y})\varepsilon_A^0(\boldsymbol{x})$ where $\boldsymbol{y}$ is a discrete variable denoting position of atoms. For more details and extension to multiple temporal scales we refer to [49]. The discrete influence function can be obtained by minimizing potential energy in a unit cell, $\Pi(u_i^0(\boldsymbol{x}) + \zeta\chi_{iA}(\boldsymbol{y})\varepsilon_A^0(\boldsymbol{x}))$, with respect to the discrete influence function $\chi_{iA}(\boldsymbol{y})$ subjected to periodic boundary conditions $\chi_{iA}(\boldsymbol{y}) = \chi_{iA}(\boldsymbol{y} + \hat{\boldsymbol{y}})$ on $\partial\Theta$ while keeping the coarse scale fields fixed over the unit cell domain. Once the influence functions are computed, the enriched quasi-continuum interpolation is given by Eq.(3), and the formulation proceeds along the lines described in [47, 48].

3. Analysis of the integration scheme

Let $\Omega^e = [0,1]$ be the domain of coarse scale elements in 1D such that $n_{uc}\Theta = 1$ where n_{uc} represents the number of unit cells in Ω^e and Θ is the size of the unit cell. Consider a typical integrand of the form $\left(c_0 + c_1 x + c_2 x^2\right) g(x)$ where $g(x)$ is a Θ-periodic function such that

$$\int_{\Theta} g(x)dx = \beta\Theta = \frac{\beta}{n_{uc}} \tag{5}$$

In this section we show that the integration error resulting from the Homogenization-Like Integration scheme is of the order $O(1/n_{uc})$.

Consider a typical integral

$$\Pi = \int_0^1 \left(c_0 + c_1 x + c_2 x^2\right) g(x)\, dx = \sum_{i=1}^{n_{uc}} \int_{\Theta_i} \left(c_0 + c_1 x + c_2 x^2\right) g(x)\, dx \tag{6}$$

To evaluate the exact integral, we utilize the mean value theorem for each unit cell domain, which gives

$$\begin{aligned} \Pi_{ex} &= \sum_{i=1}^{n_{uc}} \left[\left(c_0 + c_1 \xi_i + c_2 {\xi_i}^2\right) \int_{\Theta_i} g(x)\, dx \right] = \frac{\beta}{n_{uc}} \sum_{i=1}^{n_{uc}} \left(c_0 + c_1 \xi_i + c_2 {\xi_i}^2\right) \\ &= \beta c_0 + \beta c_1 \frac{1}{n_{uc}} \sum_{i=1}^{n_{uc}} \xi_i + \beta c_2 \frac{1}{n_{uc}} \sum_{i=1}^{n_{uc}} {\xi_i}^2 \end{aligned} \tag{7}$$

$$\text{Where } \ \xi_i \in \left[(i-1)\Theta, i\Theta\right] = \left[\frac{(i-1)}{n_{uc}}, \frac{i}{n_{uc}}\right]$$

For numerical integration, we use two Gauss points

$$\Pi_{nu} = \sum_{I=1}^{2} W_I J_I \frac{1}{|\Theta|} \int_{\Theta_I} \left(c_0 + c_1 x + c_2 x^2\right) g(x)\, dx \tag{8}$$

where

$$\begin{aligned} &W_1 = W_2 = \frac{1}{2},\ J_1 = J_2 = 1, \\ &\Theta_1 = \left[\frac{1}{2}\left(1 - \frac{1}{\sqrt{3}}\right) - \frac{1}{2n_{uc}}, \frac{1}{2}\left(1 - \frac{1}{\sqrt{3}}\right) + \frac{1}{2n_{uc}}\right], \\ &\Theta_2 = \left[\frac{1}{2}\left(1 + \frac{1}{\sqrt{3}}\right) - \frac{1}{2n_{uc}}, \frac{1}{2}\left(1 + \frac{1}{\sqrt{3}}\right) + \frac{1}{2n_{uc}}\right] \end{aligned}$$

As before, to evaluate the two integrals in (8) we use the mean value theorem

$$\begin{aligned} \Pi_{nu} &= \frac{1}{2|\Theta|} \left[\left(c_0 + c_1 \eta_1 + c_2 {\eta_1}^2\right) \int_{\Theta_1} g(x)\, dx + \left(c_0 + c_1 \eta_2 + c_2 {\eta_2}^2\right) \int_{\Theta_2} g(x)\, dx \right] \\ &= \beta c_0 + \beta c_1 \frac{1}{2}\left(\eta_1 + \eta_2\right) + \beta c_2 \frac{1}{2}\left({\eta_1}^2 + {\eta_2}^2\right) \end{aligned} \tag{9}$$

where

$$\eta_1 \in \left[\frac{1}{2}\left(1-\frac{1}{\sqrt{3}}\right)-\frac{1}{2n_{uc}}, \frac{1}{2}\left(1-\frac{1}{\sqrt{3}}\right)+\frac{1}{2n_{uc}}\right],$$
$$\eta_2 \in \left[\frac{1}{2}\left(1+\frac{1}{\sqrt{3}}\right)-\frac{1}{2n_{uc}}, \frac{1}{2}\left(1+\frac{1}{\sqrt{3}}\right)+\frac{1}{2n_{uc}}\right] \tag{10}$$

The integration error is given by

$$\begin{aligned} e &= \left|\Pi_{ex} - \Pi_{uc}\right| \\ &= \left|\beta c_1\left(\frac{1}{n_{uc}}\sum_{i=1}^{n_{uc}}\xi_i - \frac{1}{2}\left(\eta_1+\eta_2\right)\right) + \beta c_2\left(\frac{1}{n_{uc}}\sum_{i=1}^{n_{uc}}{\xi_i}^2 - \frac{1}{2}\left({\eta_1}^2+{\eta_2}^2\right)\right)\right| \\ &\le \left|\beta c_1\right|\cdot\underbrace{\left|\frac{1}{n_{uc}}\sum_{i=1}^{n_{uc}}\xi_i - \frac{1}{2}\left(\eta_1+\eta_2\right)\right|}_{A} + \left|\beta c_2\right|\cdot\underbrace{\left|\frac{1}{n_{uc}}\sum_{i=1}^{n_{uc}}{\xi_i}^2 - \frac{1}{2}\left({\eta_1}^2+{\eta_2}^2\right)\right|}_{B} \end{aligned} \tag{11}$$

The bounds for ***A*** and term ***B*** can be estimated in the closed form

$$\begin{aligned} A_{\max} &= \max\left(\left|\left(\frac{1}{n_{uc}}\sum_{i=1}^{n_{uc}}\xi_i\right)_{\max} - \left(\frac{1}{2}\left(\eta_1+\eta_2\right)\right)_{\min}\right|, \left|\left(\frac{1}{2}\left(\eta_1+\eta_2\right)\right)_{\max} - \left(\frac{1}{n_{uc}}\sum_{i=1}^{n_{uc}}\xi_i\right)_{\min}\right|\right) \\ &= \max\left(\frac{1}{n_{uc}}, \frac{1}{n_{uc}}\right) = \frac{1}{n_{uc}} \\ B_{\max} &= \max\left(\left|\left(\frac{1}{n_{uc}}\sum_{i=1}^{n_{uc}}{\xi_i}^2\right)_{\max} - \left(\frac{1}{2}\left({\eta_1}^2+{\eta_2}^2\right)\right)_{\min}\right|, \left|\left(\frac{1}{2}\left({\eta_1}^2+{\eta_2}^2\right)\right)_{\max} - \left(\frac{1}{n_{uc}}\sum_{i=1}^{n_{uc}}{\xi_i}^2\right)_{\min}\right|\right) \\ &= \max\left(\frac{1}{n_{uc}} - \frac{1}{12n_{uc}^2}, \frac{1}{n_{uc}} + \frac{1}{12n_{uc}^2}\right) = \frac{1}{n_{uc}} + \frac{1}{12n_{uc}^2} \end{aligned} \tag{12}$$

The integration error can be bounded by

$$\begin{aligned} e &\le \left|\beta c_1\right|\cdot A_{\max} + \left|\beta c_2\right|\cdot B_{\max} \\ &= \left|\beta c_1\right|\cdot\frac{1}{n_{uc}} + \left|\beta c_2\right|\cdot\left(\frac{1}{n_{uc}} + \frac{1}{12n_{uc}^2}\right) \sim O\left(\frac{1}{n_{uc}}\right) \end{aligned} \tag{13}$$

It can be seen that the integration error of the homogenization-like integration scheme is of order $O(1/n_{uc})$, and thus $e \to 0$ as $n_{uc} \to \infty$.

4. Fine-to-coarse scale transition

In this section, we show that MEPU elements degenerate to the standard finite elements with homogenized properties in case of a constant (coarse scale) strain field. We then show that continuity of average tractions and coarse scale displacements between MEPU and standard finite elements is automatically maintained for the locally constant coarse scale strain field. We then devise a patch to test the validity of the fine-to-coarse scale transitioning. We discuss the

formulation in the context of continuum enrichment, but the same procedure applies to the quasi-continuum enrichment (see numerical experiments in Section 5).

Consider the strain field obtained from Eq. (3)

$$\varepsilon_B = \varepsilon_B^0 + \left(\phi_{BA}(\boldsymbol{x})N_\alpha(\boldsymbol{x}) + B_{Bi\alpha}(\boldsymbol{x})\chi_{iA}(\boldsymbol{x})\right)a_{A\alpha} \tag{14}$$

where ϕ_{AB} is symmetric gradient of χ_{iA}

$$\phi_{ijA} = \left(\chi_{iA,j} + \chi_{jA,i}\right)/2 \rightarrow \phi_{BA} \tag{15}$$

and $B_{Bm\gamma}$ the coarse scale strain-displacement matrix defined as

$$B_{ijm\gamma} = \frac{1}{2}\left(\frac{\partial N_\gamma}{\partial x_j}\delta_{im} + \frac{\partial N_\gamma}{\partial x_i}\delta_{jm}\right) = \frac{\partial N_\gamma}{\partial x_k}I_{kmji} \rightarrow B_{Bm\gamma} \tag{16}$$

Given the constant coarse scale strain field, ε_B^0, over the unit cell domain, find $a_{A\alpha}$, such that

$$\int_\Theta \left(\phi_{BA}N_\alpha + B_{Bi\alpha}\chi_{iA}\right)D_{BC}\left[\varepsilon_C^0 + \left(\phi_{CD}N_\beta + B_{Cj\beta}\chi_{jD}\right)a_{D\beta}\right]d\Theta = 0 \tag{17}$$

The system has a unique solution since $\int_\Theta \left(\phi_{BA}N_\alpha + B_{Bi\alpha}\chi_{iA}\right)D_{BC}\left(\phi_{CD}N_\beta + B_{Cj\beta}\chi_{jD}\right)d\Theta$ is symmetric positive definite and the right hand side is nonzero.

Taking summation over the element nodes in Eq. (17) yields

$$\int_\Theta \left\{\phi_{BA}\sigma_B + \sum_\alpha \left(B_{Bi\alpha}\chi_{iA}\right)D_{BC}\left[\varepsilon_C^0 + \left(\phi_{CD}N_\beta + B_{Cj\beta}\chi_{jD}\right)a_{D\beta}\right]\right\}d\Theta = 0 \tag{18}$$

Due to the PU property, $\sum_\alpha B_{Bi\alpha} = 0$, we get

$$\sum_\alpha \left(B_{Bi\alpha}\chi_{iA}\right) = 0 \tag{19}$$

which yields

$$\int \phi_{BA}D_{BC}\left[\varepsilon_C^0 + \left(\phi_{CD}N_\beta + B_{Cj\beta}\chi_{jD}\right)a_{D\beta}\right]d\Theta = 0 \tag{20}$$

Since χ_{jD} is a weak form solution of Eq. (2) satisfying, $\int_\Theta \phi_{BA}D_{BC}\left(I_{CD} + \phi_{CD}\right)d\Theta = 0$, Eq. (20) can be written as:

$$\int_\Theta \begin{pmatrix} \underbrace{\phi_{BA}D_{BC}I_{CD}\varepsilon_D^0 + \phi_{BA}D_{BC}\phi_{CD}\varepsilon_D^0}_{\text{Unit Cell equation}} \\ -\phi_{BA}D_{BC}\phi_{CD}\varepsilon_D^0 + \phi_{BA}D_{BC}\left(\phi_{CD}N_\beta + B_{Cj\beta}\chi_{jD}\right)a_{D\beta} \end{pmatrix} d\Theta = 0 \tag{21}$$

which can be further simplified as

$$\int_{\Theta}\left[\phi_{BA}D_{BC}\phi_{CD}\left(N_{\beta}a_{D\beta}-\varepsilon_{D}^{0}\right)+\phi_{BA}D_{BC}B_{Cj\beta}\chi_{jD}a_{D\beta}\right]d\Theta=0 \tag{22}$$

It can be seen that if $a_{D\beta}\equiv a_D=\varepsilon_D^0 \quad \forall\beta$ then $N_\beta a_{D\beta}=\sum_\beta N_\beta a_D = a_D=\varepsilon_D^0$ and the first term in Eq. (22) vanishes. Moreover, $B_{Cj\beta}\chi_{jD}a_{D\beta}=\sum_\beta B_{Cj\beta}\chi_{jD}a_D=0$, and thus $a_{D\beta}=\varepsilon_D^0 \quad \forall\beta$ is the solution of Eq. (22). The resulting stress is given by $\sigma_B=D_{BC}\left(I_{CD}+\phi_{CD}\right)\varepsilon_D^0$. The nonlocal or average stress becomes $\bar{\sigma}_B=\underbrace{\int_{\Theta}D_{BC}\left(I_{CD}+\phi_{CD}\right)d\Theta}_{\bar{D}_{BC}}\varepsilon_D^0\equiv\bar{D}_{BC}\varepsilon_D^0$, which is identical to the stress obtained by standard finite element with homogenized properties. The upshot of this finding is that at the interface between the MEPU and standard finite elements with homogenized properties continuity of average tractions is maintained. Moreover, continuity of coarse scale displacements $N_\beta(\boldsymbol{x})d_{i\beta}$ is automatically enforced at the interface, whereas the enrichment $\chi_{iA}(\boldsymbol{x})N_\alpha(\boldsymbol{x})a_{A\alpha}$ is allowed to be discontinuous. We will refer to such continuity condition, which enforces continuity of average tractions and coarse scale displacements, as *coarse scale continuity*.

We now consider a patch of elements where a single MEPU element is surrounded by standard finite elements with homogenized material properties. Both structured and unstructured meshes are considered as shown in Figure 2.

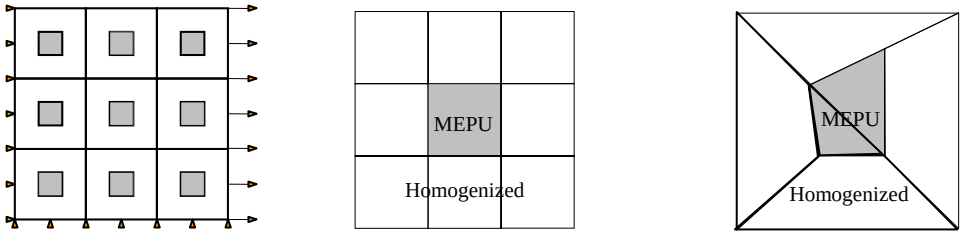

Figure 2: The patch test for interfaces

For comparison, we also consider the formulation where *total* displacements across the interface are enforced to be continuous. We will refer to such continuity formulation as *fine scale continuity*. Figure 3 shows the displacement field u_2 obtained by subjecting the patch of elements to Dirichlet boundary conditions corresponding to the constant coarse scale strain field ε_{11}^0 .

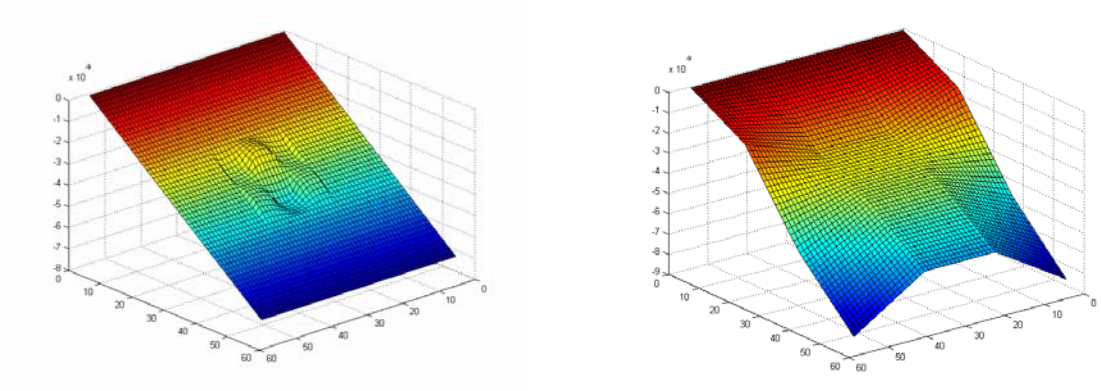

a. Coarse-scale continuity b. Fine-scale continuity

Figure 3: Displacements u_2 obtained from ε_{11}^0.

The relative error $\left|e^{ref} - e^{FEM}\right| / e^{ref}$ in strain energy density, $e = \overline{\sigma}_A \varepsilon_A^0 / 2$, is plotted in Figure 4. It can bee seen that the formulation enforcing fine scale displacement continuity gives rise to large errors, whereas in case of *coarse scale continuity* the solution of the strain energy density is exact.

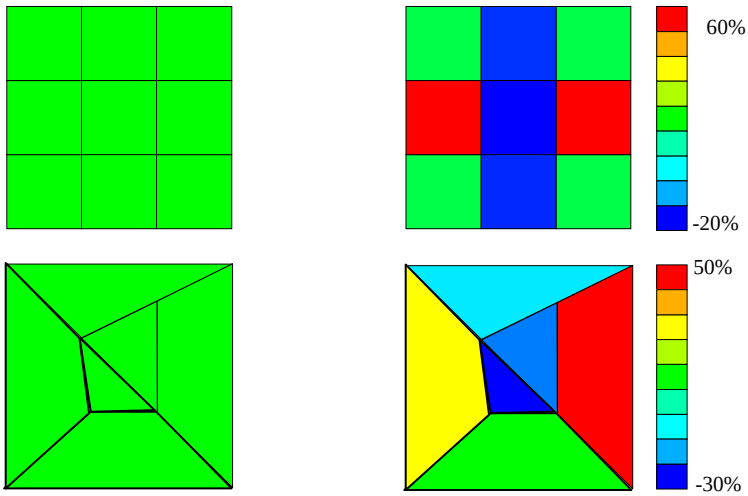

a. Coarse-scale continuity b. Fine-scale continuity

Figure 4: Errors in relative strain energy density $e = \overline{\sigma}_A \varepsilon_A^0 / 2$

5. Numerical examples

In this section, MEPU is tested for various continuum and quasi-continuum fracture problems. We start with a two-dimensional coarse scale configuration shown in Figure 5. The uniform displacement boundary condition is applied along the top and bottom edges of the plate. Due to symmetry, only the upper half of the plate is analyzed.

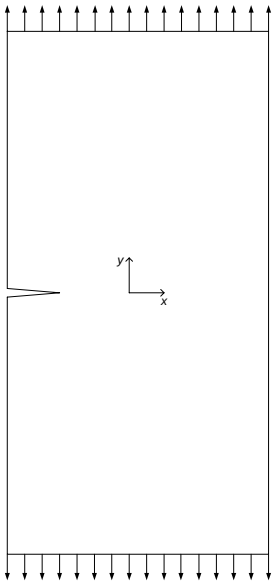

Figure 5: Configuration for the two-dimensional continuum fracture problem

We consider a unit cell with a square inclusion as shown in Figure 6. The phase properties of the fine scale constituents are as follows. Inclusion : Young's Modulus = 60GPa, Poisson's ratio = 0.2. Matrix: Young's Modulus = 2GPa, Poisson's ratio = 0.2. The coarse scale domain contains 16 by 16 unit cells. The reference mesh is shown in Figure 6.

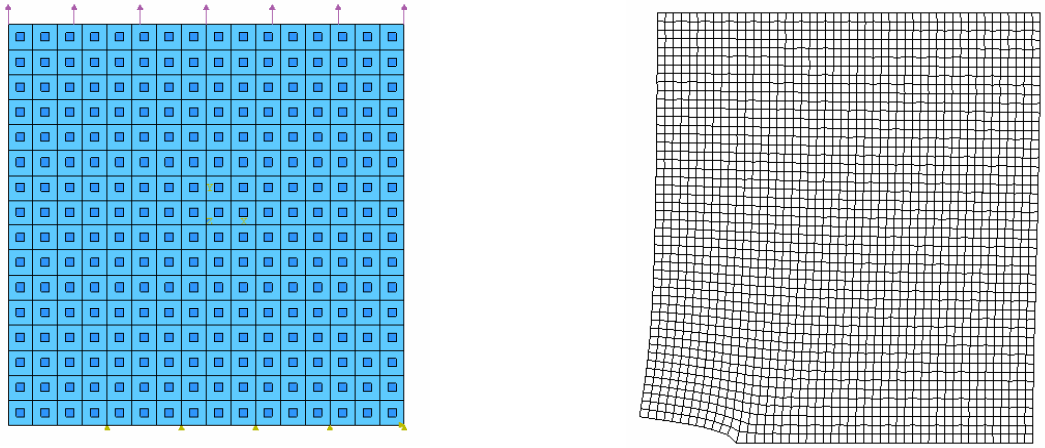

a. Undeformed configuration b. Deformed configuration

Figure 6: Reference mesh for the two-dimensional contimum fracture problem

For comparison, three methods are investigated: (i) homogenization (HOMO), which uses standard finite element with homogenized properties, (ii) MEPU, and (iii) combination of HOMO and MEPU, where MEPU is used around the crack tip and HOMO elsewhere. Both structured and unstructured meshes are considered. All the meshes are shown in Figure 7. The enrichment functions, $\chi_{A\alpha}$, are obtained using finite element solution of the corresponding unit cell problem (2).

The results of mode-I stress intensity factor are summarized in Table 1. The stress intensity factors were evaluated using virtual crack closure integral method [50].

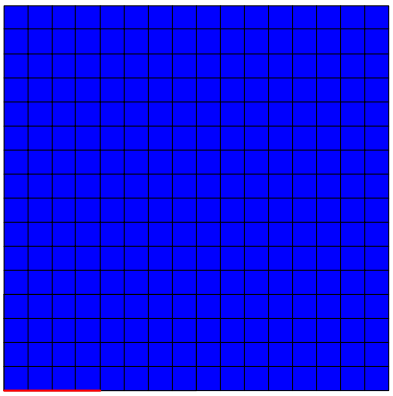

a. HOMO (MEPU) Structured Mesh

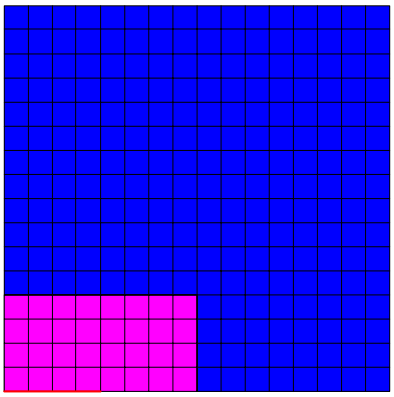

b. MEPU_HOMO Structured Mesh

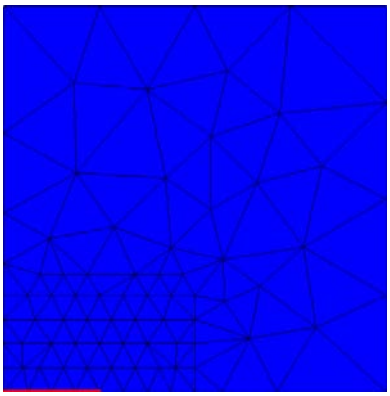

c. HOMO (MEPU) Unstructured Mesh

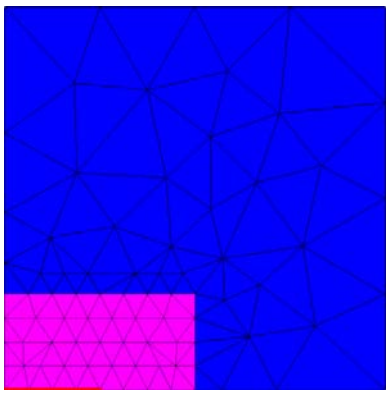

d. MEPU_HOMO Unstructured Mesh

Figure 7: Homogenized and MEPU meshes for the two-dimensional contimum fracture problem

Table 1: Mode I stress intensity factor for the two-dimensional contimum fracture problem

Methods	Structured Mesh		Unstructured Mesh	
	K	Error	K	Error
HOMO	5.4377E+07	3.75%	5.2848E+07	6.45%
MEPU_HOMO	5.5872E+07	1.10%	5.3471E+07	5.35%
MEPU	5.6290E+07	0.36%	5.3956E+07	4.49%
REF	5.6493E+07	-	5.6493E+07	-

For rate of convergence studies, three meshes shown in Figure 8 were considered. Table 2 gives the relative error in the stress intensity factor obtained by using three different methods. The logarithm of error is plotted in Figure 9.

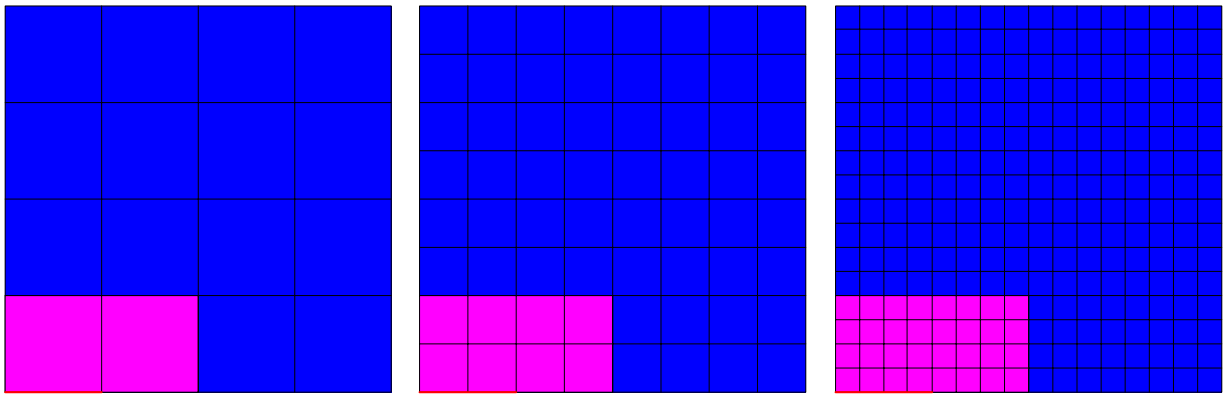

a. Coarse Mesh b. Fine Mesh c. Very Fine Mesh

Figure 8: Mesh refinement for the two-dimensional contimum fracture problem

Table 2: The relative error in mode-I stress intensity factor for two-dimensional contimum fracture problem

Methods\Mesh	Coarse	Fine	Very fine
MEPU	76.11%	32.74%	0.36%
MEPU_HOMO	74.48%	30.86%	1.10%
HOMO	98.28%	34.72%	3.75%

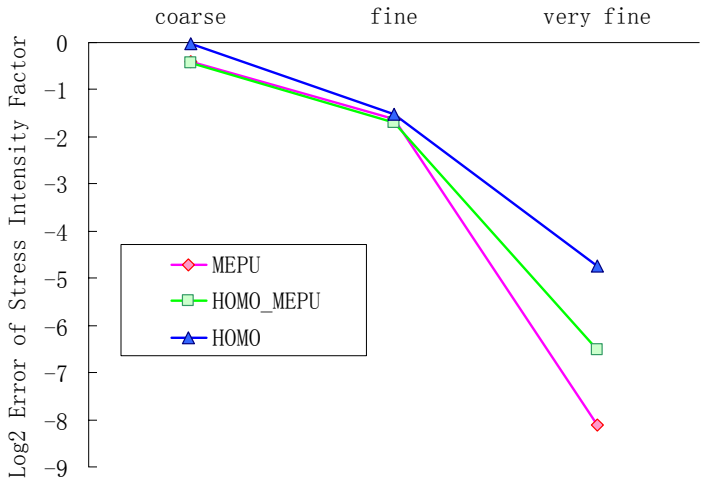

Figure 9: Convergence of mode-I stress intensity factor

In the next set of numerical examples, we consider a three-dimensional fracture problem with two different unit cells. The former is a fibrous composite with the following phase properties. Fiber: Young's modulus = 379GPa, Poisson's ratio = 0.21. Matrix: Young's modulus = 69GPa, Poisson's ratio = 0.33. The problem configuration and the corresponding unit cell are shown in Figure 10. The latter is a satin weave [51]. The phase properties of the weave constituents are as follows. Blackglas Matrix: Young's modulus = 69GPa, Poisson's ratio = 0.33. Bundle phase: Young's modulus = 679GPa, Poisson's ratio = 0.21. The unit cell shown in Figure 11 is discretized with 1566 elements.

In general, it is not feasible to use a discretization scheme with grid spacing comparable to the scale of spatial heterogeneities. To obtain the reference solution the satin weave problem

considered in Figure 12 was discretized with 626400 standard elements. On the hand, MEPU requires, only 400 elements, but each element has additional 6 degrees-of-freedom per node.

The results of the strain energy release rate for the two unit cells are summarized in Table 3.

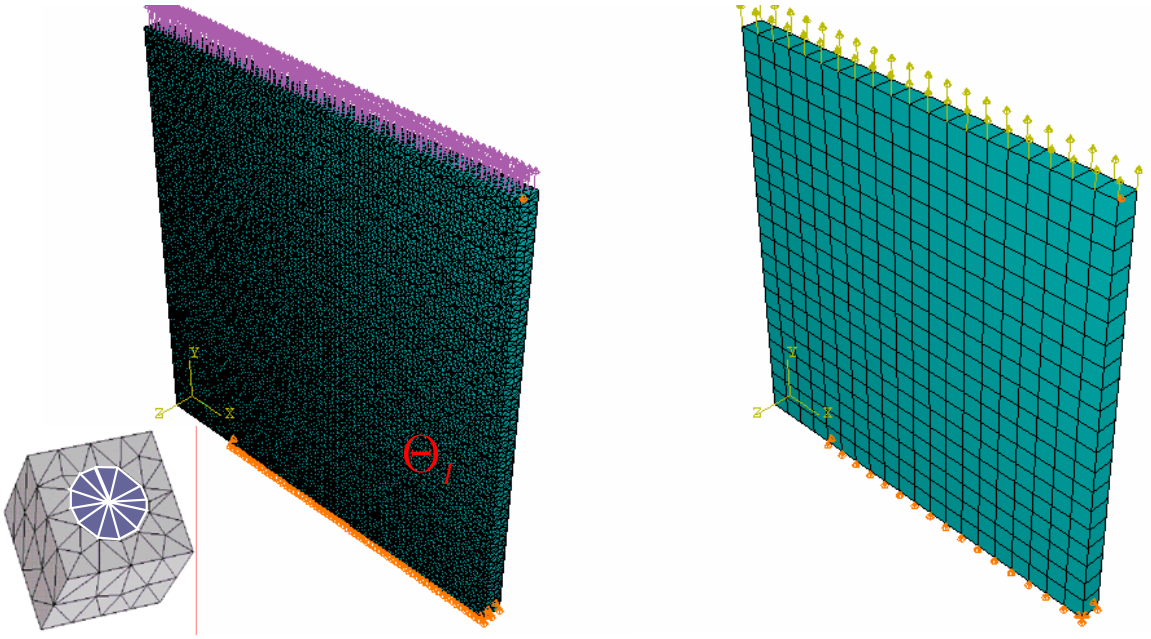

a. Reference Mesh b. MEPU (HOMO) Mesh

Figure 10: Three-dimensional contimum fracture problem for fibrous composite and the corresponding unit cell

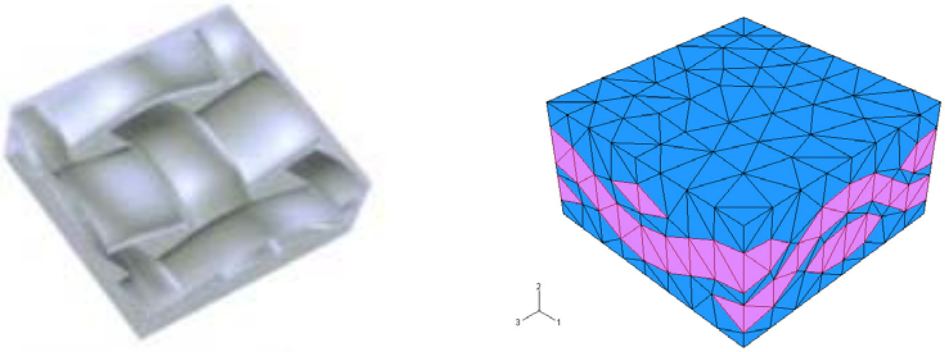

a. Geometric model b. Finite element mesh

Figure 11: Woven unit cell [51]

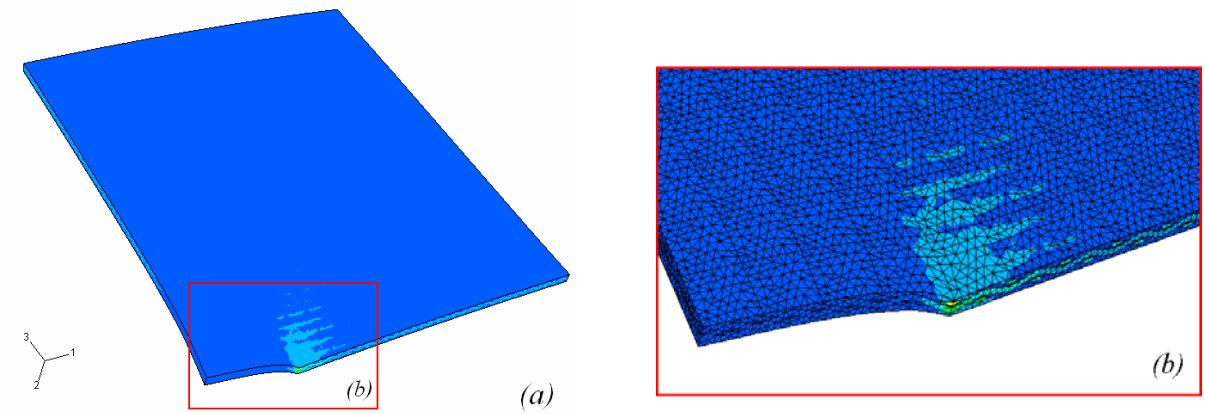

Figure 12: Three dimensional contimum fracture problem for woven composites

Table 3: Strain energy release rate G of three dimensional contimum fracture problem

Methods	Fibrous composites		Woven composites	
	G	Error	G	Error
HOMO	2.0564	4.61%	28.0564	4.16%
MEPU	1.9991	1.69%	27.4670	1.97%
REF	1.9659	-	26.9371	-

In the final numerical example, we consider a discrete (atomistic) model problem in two dimensions. The problem configuration is shown in Figure 13. Atoms are assumed to interact only with their nearest neighbors in horizontal, vertical and diagonal directions. The interatomic interactions are assumed to be stronger for the four atoms positioned at the center of the unit cell (black-black connections) and weaker for the remaining atomic pairs (blue-blue and blue-black connections) as shown in Figure 13. The quadratic approximation of the Lennard-Jones potential

$$E_a(r) = -\varepsilon_1 + \frac{1}{2}a\left(r - r_0^1\right)^2,\ E_b(r) = -\varepsilon_2 + \frac{1}{2}b\left(r - r_0^2\right)^2 \tag{23}$$

has been employed, where $r_0^k\,(k=1,2)$ are the interatomic distances at the equilibrium; a and b are constants defined by: $a = \frac{36\sqrt[3]{4}\varepsilon_1}{\sigma_1^2}$ and $b = \frac{36\sqrt[3]{4}\varepsilon_2}{\sigma_2^2}$, where $\sigma_1 = 3.405\times10^{-10}$, $\varepsilon_1 = 1.6572\times10^{-21}$; $\sigma_2 = 3.405\times10^{-10}$, $\varepsilon_2 = 1.6572\times10^{-20}$.

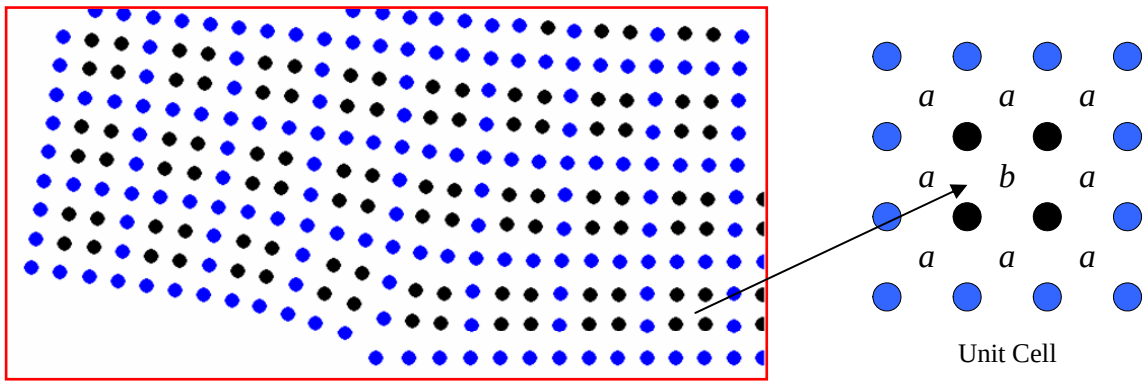

Figure 13: Two-dimensional quasicontinuum fracture problem and the corresponding unit cell

The results of the potential energy and the energy release rate obtained using molecular mechanics (the reference solution), MEPU and Quasi-Continuum method based on the Born rule are summarized in Table 4.

Table 4: Potential energy E and Potential energy release rate G of two dimensional atomic fracture problem

Methods	Potential energy		Potential energy release rate	
	E	Error	G	Error
QC	1.75	90.42%	0.041460	89.88%
MEPU	0.925	0.65%	0.021139	3.18%
REF	0.919	-	0.021835	-

It can be seen that MEPU provides a very accurate solution for both the potential energy and the energy release rate, whereas quasi-continuum assuming Born rule behaves poorly for problems involving heterogeneous potentials.

6. Conclusions and Future Research Directions

Multiscale Enrichment based on Partition of Unity presented in this manuscript provides a considerable improvement over classical mathematical homogenization theory and quasi-continuum for continuum and discrete systems, respectively. One of its main attractions stems from the ease of implementation into most of the commercial software packages. Any commercial code that allows for adding user-defined elements with *arbitrary* number of degrees-of-freedom per node can be used for implementation. MEPU can be easily implemented into the quasi-continuum framework by replacing the Born rule with appropriate enrichment functions. Homogenization error estimators [52,53] can be utilized to identify the location where enrichment is needed.

So far, the method has been studied assuming small deformations, harmonic potentials and steady state conditions. It remains to be seen whether the *coarse scale continuity conditions* set fourth in this paper are sufficient to avoid spurious wave reflections at the atomistic/continuum interface or whether some sort of overlapping as described in [54] is needed.

Wave dispersion is another issue, which needs a careful examination. Existing methodologies (see for example [55,56,57]) are based on continuum (or quasi-continuum) enrichment. It remain to be seen if higher order enrichment functions P_{ijmn} (18 functions in 3D corresponding to the gradients of the coarse scale strain field), which play a central role in the formulation of existing dispersive models, have to be added to enrich the element kinematics. With increase in the order of enrichment functions, the polynomial order of the coarse scale fields may have to be appropriately increased to let the unit cell “experience” higher order coarse fields over its domain. Thus, it may be advantageous to use different polynomial order of the shape (support) functions in the first and second term of Eq. (3).

These are just few of the issues that will be addressed in our future research work.

Acknowledgment

This work was supported by the National Science Foundation under grants CMS 0303902 and CMS 0310596.

7. References

1 C.D. Mote, “Global-Local Finite Element Method,” *International Journal for Numerical Methods in Engineering*, Vol. 3, pp. 565-574, 1971.

2 A. K. Noor, “Global-Local methodologies and their application to nonlinear analysis,” *Finite Elements in Analysis and Design*, Vol. 2, pp. 333-346, 1986.

3 S. B. Dong, Global-Local Finite Element Methods,” in State-of-the-Art Surveys on Finite Element Technology, eds. A. K. Noor and W.D. Pilkey, ASME, pp. 451-474, 1983.

4 L. N. Gifford and P. Hilton, “Stress Intensity Factors by Enriched Finite Elements,” Engineering Fracture Mechanics,” Vol. 10, pp. 485-496, 1978.

5 T. Belytschko, J. Fish, and A. Bayliss, “The spectral overlay on the finite element solutions with high gradients,” *Computer Methods in Applied Mechanics and Engineering*,” Vol. 81, pp. 71-89, (1990).

6 T. Belytschko, J. Fish and B.E. Engelman, “A finite element with embedded localization zones,” *Computer Methods in Applied Mechanics and Engineering*, Vol. 70, (1988), pp. 59 - 89.

7 J. Fish and T. Belytschko, “Elements with embedded localization zones for large deformation problems,” *Computers and Structures*, Vol. 30, No. 1/2, (1988), pp. 247-256.

8 T. Belytschko and J. Fish, "Embedded hinge lines for plate elements,” *Computer Methods in Applied Mechanics and Engineering*, Vol. 76, No. 1, (1989), pp. 67-86.

9 F. Armero and K.Garikipati, “An analysis of strong discontinuities in multiplicative finite strain plasticity and their relation with the numerical simulation of strain localization,” *International Journal of Solids and Structure*s, Vol. 33, pp. 2863-2885, 1996.

10 J. C. Simo, J. Oliver, and F. Armero, “An analysis of strong discontinuities induced by strain-sofetening in rate-independent inelastic solids,” *Computational Mechanics*, Vol. 12, pp. 277-296, 1993.

11 T. J. R. Hughes, “Multiscale phenomena: Green’s functions, the Dirichlet to Neumann formulation, subgrid scale models, bubbles and the origin of stabilized methods,” *Computer Methods in Applied Mechanics and Engineering*, Vol. 127, pp. 387-401. 1995.

12 F. Brezzi and A. Russo, “Choosing bubbles for advection-diffusion problems,” *Math. Models Methods Appl. Sci.*, Vol. 4, pp. 571–587, 1994.

13 L. P. Franca and A. Russo, “Approximation of the Stokes problem by residual-free macro bubbles,” *J. Numer. Math*., Vol. 4, pp. 265–278, 1996.

14 K. Garikipati and T.J.R. Hughes, “A study of strain localization in a multiple scale framework—the one dimensional problem,” *Computer Methods in Applied Mechanics and Engineering*, Vol. 159, pp. 193–222, 1998.

15 K. Garikipati and T.J.R. Hughes, “A variational multiscale approach to strain localization—formulation for multidimensional problems,” *Computer Methods in Applied Mechanics and Engineering*, Vol. 188, pp. 39– 60, 2000.

16 I. Babuska, “Homogenization and Application. Mathematical and Computational Problems,” *Numerical Solution of Partial Differential Equations – III, SYNSPADE*, eds. B Hubbard, Academic Press, 1975.

17 A. Benssousan, J.L. Lions and G. Papanicoulau, Asymptotic Analysis for Periodic Structures, North-Holland, 1978.

18 J. M. Guedes and N. Kikuchi, “Preprocessing and postprocessing for materials based on the homogenization method with adaptive finite element methods,” *Computer Methods in Applied Mechanics and Engineering*, Vol. 83, pp. 143-198, 1990.

19 J. Fish, "The s-version of the finite element method," *Computers and Structures*, Vol. 43, No. 3, pp. 539-547, 1992.

20 J. Fish and S.Markolefas, "Adaptive s-method for linear elastostatics," *Computer Methods in Applied Mechanics and Engineering*, Vol. 103, pp. 363-396, 1993.

21 J. Fish and S.Markolefas, R.Guttal and P.Nayak, "On adaptive multilevel superposition of finite element meshes," *Applied Numerical Mathematics*, Vol 14., pp. 135-164, 1994.

22 J.W. Park, J.W. Hwang and Y.H. Kim, “Efficient finite element analysis using mesh superposition technique,” *Finite elements in analysis and design*, Vol. 39, pp. 619-638, 2003.

23 J. Fish, "Hierarchical modeling of discontinuous fields," *Communications in Applied Numerical Methods*, Vol. 8, pp. 443-453, 1992.

24 J. Fish, N.Fares and A.Nath, "Micromechanical elastic cracktip stresses in a fibrous composite," *International Journal of Fracture*, Vol. 60, pp. 135-146, 1993.
25 J. Fish and A. Wagiman, "Multiscale finite element method for heterogeneous medium," *Computational Mechanics: The International Journal*, Vol. 12, pp. 1-17, 1993.
26 J.Fish and S.Markolefas, "The s-version of the finite element method for multilayer laminates," *International Journal for Numerical Methods in Engineering*, Vol. 33, no. 5, pp. 1081-1105, 1992.
27 D.H. Robbins and J.N. Reddy, "Variable kenematic modeling of laminated composite plates," *International Journal for Numerical Methods in Engineering*, Vol. 39, pp. 2283-2317, 1996.
28 N. Takano, M. Zako, and M. Ishizono, "Multi-scale computational method for elastic bodies with global and local heterogeneity," *J. Computer-Aided Material Design*, Vol. 7, pp. 111-132, 2000.
29 J. Fish and V.Belsky, "Multigrid method for a periodic heterogeneous medium. Part I: Convergence studies for one-dimensional case," Comp. Meth. Appl. Mech. Engng., Vol. 126, pp. 1-16, (1995).
30 J. Fish and V. Belsky, "Multigrid method for a periodic heterogeneous medium. Part 2: Multiscale modeling and quality control in mutidimensional case," *Computer Methods in Applied Mechanics and Engineering*, Vol. 126, 17-38, 1995.
31 J.Fish, A.Suvorov and V.Belsky,'Hierarchical Composite Grid Method for Global-Local Analysis of Laminated Composite Shells,' *Applied Numerical Mathematics*, Vol. 23, pp.241-258, (1997).
32 J. Fish and W. Chen, "Discrete-to-Continuum Bridging Based on Multigrid Principles," *Computer Methods in Applied Mechanics and Engineering*, Vol. 193, pp. 1693-1711, 2004.
33 T. Belytschko and T. Black, "Elastic crack growth in finite elements with minimal remeshing," *International Journal for Numerical Methods in Engineering*, Vol. 45, No. 5, pp. 601-620, 1999.
34 N. Moës, J. Dolbow and T. Belytschko, A finite element method for crack growth without remeshing, *International Journal for Numerical Methods in Engineering*, Vol. 46, No. 5, pp. 131-150, 1999.
35 T. Belytschko, N. Moës, S. Usui, C. Parimi, "Arbitrary discontinuities in finite element," *International Journal for Numerical Methods in Engineering*, Vol. 50, pp. 993-1013, 2001.
36 T. Strouboulis, I. Babuska and K. Copps, "The generalized finite element method: An example of its implementation and illustration of its performance," *International Journal for Numerical Methods in Engineering*, Vol. 47, pp. 1401-1417, 2000.
37 T. Strouboulis, I. Babuska and K. Copps, "The generalized finite element method," *Computer Methods in Applied Mechanics and Engineering*, Vol. 190, pp. 4081-4193, 2001.
38 I. Babuska, G. Caloz and J. E. Osborn, "Special finite element methods for a class of second order elliptic problems with rough coefficients," *SIAM. J. Numer. Anal*., Vol. 4, pp. 945-981, 1994.
39 I. Babuska and J.M. Melenk, "The partition of unity finite element method: Basic theory and applications," *Computer Methods in Applied Mechanics and Engineering*, Vol. 139, pp. 289-314, 1996.
40 J. T. Oden, I. Babuska, C.E. Baumann, "A discontinuous hp finite element method for diffusion problems," Journal of Computational Physics, Vol. 146, pp. 1-29, 1998.
41 S. S. Collis and Y. Chang, "The DG/VMS method for unified turbulence simulation," AIAA paper 2002-3124, 2002.
42 G.J. Wagner and W.K. Liu, "Coupling of atomistic and continuum simulations using a bridging scale decomposition," *Journal of Computational Physics*, Vol. 190, pp. 249-274, 2003.
43 D.K. Datta, R.C. Picu and M.S. Shephard, "Composite Grid Atomistic Continuum Method: An adaptive approach to bridge continuum with atomistic analysis," to appear in *International Journal for Multiscale Computational Engineering*, 2004.
44 C. Farhat, I. Harari, and L.P. Franca, "The discontinuous enrichment method," *Computer Methods in Applied Mechanics and Engineering*, Vol. 190, No. 48, pp. 6455-6479, 2001.
45 J. Chessa, H.W. Wang and T. Belytschko, "On the construction of blending elements for local partition of unity enriched finite elements," *International Journal for Numerical Methods in Engineering*, Vol. 57, No. 7, pp. 1015-1038, 2003.
46 G. J. Wagner, N. Moes, W.K. Liu, and T. Belytschko, "The Extended Finite Element Method for Rigid Particles in Stokes Flow," *International Journal for Numerical Methods in Engineering*, Vol. 51, pp. 293-310, 2001.
47 E. B. Tadmor, M. Ortiz, and R. Phillips, "Quasicontinuum analysis of defects in solids" *Phil. Mag. A* , Vol. 73, pp. 1529-1564, 1996.

48 R. E. Miller and E.B. Tadmor, "The Quasicontinuum Method: Overview, Applications and Current Directions", J. of Computer-Aided Materials Design, Vol. 9, pp. 203-209, 2002.
49 J. Fish and C. Schwob, “Towards Constitutive Model Based on Atomistics,” *International Journal of Multiscale Computational Engineering*, Vol. 1 pp. 43-56, 2003.
50 E. F. Rybicki and M. F. Kanninen, “A Finite Element Calculation of Stress Intensity Factors by a Modified Crack Closure Integral,” *Engineering Fracture Mechanics*, Vol. 9, pp. 931-938, 1977.
51 R. Wentorf, R. Collar, M.S. Shephard, J. Fish, “Automated Modeling for Complex Woven Mesostructures,” *Computer Methods in Applied Mechanics and Engineering*, Vol. 172, pp. 273-291, 1999.
52 J.Fish, P.Nayak, and M.H.Holmes, “Microscale Reduction Error Indicators and Estimators for a Periodic Heterogeneous Medium,” *Computational Mechanics: The International Journal*, Vol. 14, pp. 1-16, 1994.
53 J.T. Oden, and I. Zohdi, “Analysis and Adaptive Modeling of Highly Heterogeneous Elastic Structures”, *Computer Methods in Applied Mechanics and Engineering*, Vol. 148, No. 3-4, pp. 367-391, 1997.
54 T. Belytschko and S. P. Xiao, “Coupling methods for continuum model with molecular model,” *International Journal for Multiscale Computational Engineering*, Vol. 1, p. 115-126, 2003.
55 W. Chen W. and J. Fish, “A dispersive model for wave propagation in periodic heterogeneous media based on homogenization with multiple spatial and temporal scales,” *J. Applied Mechanics, Transaction of the ASME*, Vol. 68, pp. 153-161, 2001.
56 J. Fish, W. Chen W. and G. Nagai, “Non-local dispersive model for wave propagation in heterogeneous media: one-dimensional case *International Journal for Numerical Methods in Engineering*, Vol. 54, pp. 331-346, 2000.
57 J. Fish, W. Chen W. and G. Nagai, “Non-local dispersive model for wave propagation in heterogeneous media: multi-dimensional case,” *International Journal for Numerical Methods in Engineering*, Vol. 54, pp. 347-36, 2000.